

Gregory A. HOPE*, Ronald WOODS* and Kym WATLING*

SURFACE ENHANCED RAMAN SCATTERING SPECTROELECTROCHEMICAL STUDIES OF MINERAL PROCESSING

Received March 15, 2002, reviewed, accepted May 22, 2002

The application of *in situ* surface enhanced Raman scattering (SERS) spectroscopy to aspects of mineral processing is discussed. In the study of flotation systems, SERS has been used to characterise the species formed on coinage metal surfaces over a range of controlled potentials for ethyl, *i*-propyl, *i*-butyl and *i*-amyl xanthates, for *O*-isopropyl-*N*-ethylthionocarbamate (IPETC), for 2-mercaptobenzothiazole (MBT), and for diisobutyl dithiophosphinate (DIBDTPI). For each collector, adsorption occurs *via* charge transfer to form a metal-sulfur bond and, in situations in which the reversible potential for the formation of the bulk phase is known, at underpotentials. The dissolution of silver in basic solutions containing cyanide has been shown to be inhibited by MBT and by DIBDTPI as a result of the chemisorption of the collector species. In hydrometallurgy, SERS has been applied to the investigation of gold leaching. Changes in the surface species that occur during gold cyanidation as the potential is varied have been identified from SERS spectra recorded in real time on voltammograms. In electrometallurgy, SERS investigations of copper electrodeposition from sulfuric acid solutions have shown that a transient surface sulfate species is involved in the plating process.

Key words: Spectroelectrochemistry, Raman spectroscopy, collector adsorption, gold leaching, copper electrodeposition.

INTRODUCTION

Froth flotation, oxidative leaching, and electrowinning and refining are important unit processes in the winning of metal values from sulfide mineral ores. All these processes have electrochemical bases and are amenable to study using electrochemical concepts and techniques. Surface species play an important role in determining the efficacy of each of these processes and, whereas electrochemical techniques provide valuable information on the kinetics and mechanisms of processes occurring at the

*School of Science, Griffith University, Nathan, Queensland 4111, Australia

solid/solution interface, they lack the molecular specificity required to give unequivocal identification of species formed at electrode surfaces. For this reason, a number of *in situ*, and *ex situ* spectroscopies have been applied to augment electrochemical approaches and provide information on the elemental and molecular composition, the atomic geometry, and the electronic structure of the interface. The spectroelectrochemical techniques that have been most widely applied to mineral processing systems have involved Fourier transform infrared (FTIR) spectroscopy and X-ray photoelectron spectroscopy (XPS). These methods have provided valuable information on the identity of surface species but each has limitations. XPS is an *ex situ* technique and the surface composition can relax in the time elapsed between removal from potential control in the electrochemical cell and recording of photoelectron spectra (Buckley and Woods, 1996). A similar situation arises with FTIR when it is performed *ex situ*. FTIR can be carried out *in situ*, but the sample has to be in contact with, or within a few microns of the cell window, due to water being a strong absorber of infrared radiation.

Raman spectroscopy is complementary to infrared; both techniques give spectra resulting from transitions between the vibrational energy levels of molecules, but different selection rules apply. Raman has the advantage over infrared techniques that the incident and scattered beams can have wavelengths in the region that is not adsorbed strongly by water and in which glass is transparent. Thus, *in situ* investigations in aqueous media can be carried out using conventional glass cells. In addition, Raman spectroscopy has excellent spectral range (100 to 4000 cm^{-1}) and resolution (1 cm^{-1}) and dynamic response (< ns). On the debit side, it has a lower sensitivity for most systems. In general, only one incident photon in $\sim 10^{10}$ undergoes Raman scattering; most photons experience Rayleigh scattering in which the incident and scattered photons have the same energy. Nevertheless, the sensitivity of modern Raman spectrometers allows this technique to be applied to a wide range of problems associated with mineral processing. These include the identification of minerals, of reaction products, and of species in aqueous solution and in molten salts.

The phenomenon of surface enhanced Raman scattering (SERS) was first demonstrated by Fleischmann et al in 1973. It is applicable most usefully to adsorption on the coinage metals, copper, silver and gold. It involves a remarkable enhancement of the scattering intensity (by $\sim 10^4$ to 10^6) of species that are adsorbed on, or are microscopically close to, appropriately roughened surfaces. Silver has the widest spectral region of SERS activity, extending from blue light through to the infrared, while copper and gold are only active when irradiated with red through near infrared light. SERS generally allows surface layers at the sub-monolayer level to be characterized. Roughening electrode surfaces to generate SERS usually involves the application of oxidation-reduction potential cycling (ORC) in chloride or sulfate media. The resulting surface contains features with sizes of up to the wavelength of visible light.

In principle, SERS can also be applied to mineral surfaces by “decorating” the mineral surface with colloidal metal particles. These can be applied by either simply dipping a specimen of the mineral into the colloidal suspension, or applying a small quantity of the suspension to the surface, prior to beginning the experiment.

Raman spectroscopy is a powerful approach that is now included in the armory that metallurgists can apply to elucidating problems. In the present paper, we discuss our recent SERS investigations into flotation, hydrometallurgy and electrometallurgy.

RAMAN SPECTROSCOPY

Griffith University has two Raman spectrometers for spectroelectrochemical and mineralogical studies. One is a System 100 Renishaw Raman Spectrograph (Multi Channel Compact Raman Analyser) that has a rotary encoded grating stage, and an internal two stage Peltier cooled ($-70\text{ }^{\circ}\text{C}$) CCD detector. The spectral resolution is 5 cm^{-1} and the wavenumber resolution 1 cm^{-1} . The incident radiation is conveyed from the laser to the spectrometer through a fibre optic Raman probe. The other spectrometer is a Renishaw RM2000 Raman spectrometer equipped with a computer controlled stage and a Leica metallurgical microscope incorporating a range of objectives. The FWHM of silicon calibration band at 520 cm^{-1} was 5 cm^{-1} and the wavenumber resolution was 1 cm^{-1} . This instrument has the capability of imaging and mapping surfaces and hence can determine spatial variations in the coverage of surface species. Incident laser radiation is available of 633 nm, 514.5 nm, 442 nm and 325 nm. FT-Raman spectrometers are also accessible for research purposes.

Most spectroelectrochemical studies we have carried out used an electrochemical cell constructed of borosilicate glass with a flat window at one end. For experiments with copper and gold, the working electrode was mounted on an assembly constructed from PTFE and was positioned close to the window. It follows the design devised by Fleischmann et al. (1990). Copper and gold electrodes of 6 mm diameter were prepared from metal of 99.99% purity. With copper, the surface was electrochemically roughened prior to obtaining SERS spectra by oxidation-reduction cycling in $2\text{ mol dm}^{-3}\text{ H}_2\text{SO}_4$. This procedure involved the application of 4-5 cycles between -0.3 V and 0.7 V with a polarisation period of approximately 30 s before reversing the polarity. With gold, oxidation-reduction cycling was carried out between -0.3 and 1.2 V in $1\text{ mol dm}^{-3}\text{ KCl}$ acidified with HCl. A cell of similar design was used for silver, but the working electrode was a silver flag attached to a silver wire. This design allowed the electrode to be cleaned by heat treatment. The electrode was heated in a furnace at $450\text{ }^{\circ}\text{C}$ for 16 h to remove any organic species and then roughened by applying oxidation-reduction cycling in $1\text{ mol dm}^{-3}\text{ KCl}$ acidified with HCl between potentials of -0.2 and 0.6 V after initially reducing at -0.5 V .

In addition to spectra recorded *in situ* under potential control, spectra have been recorded on emersed electrodes and on electrodes *ex situ*. For measurements on emersed electrodes, spectra were recorded after the solution had been drained from the

cell. The removal of solution was carried out under a constant flow of nitrogen to avoid ingress of oxygen from the atmosphere during emersion and the recording of spectra. In the last situation, the electrode was removed from the cell and washed with pure water to remove any cell solution from the electrode surface prior to examination in the spectrometer. This procedure provided information on the tenacity of attachment of species to the electrode surface as well as the identity of adsorbates.

In some experiments, Raman spectra were recorded sequentially on a potential step or scan. With the Renishaw spectrometers, the Grams 32 and 3D software allows sequential spectra to be stored as separate files and viewed as a 'movie' or a 3D image.

FROTH FLOTATION

The key chemical step in the flotation process is the adsorption of the organic collector on selected mineral surfaces and it is now well established that the interaction of thiol collectors with sulfide minerals is electrochemical in nature. It was originally proposed by Nixon (1957) that interaction occurred by an anodic process involving the collector being coupled with a cathodic process which is usually the reduction of oxygen. Professor Andrzej Pomianowski was one of the pioneers of the application of electrochemical techniques to characterizing collector adsorption. He and his co-workers carried out cyclic voltammetric studies of ethyl xanthate on mercury (Pomianowski, 1967), on chalcocite (Kowal and Pomianowski, 1973) and on copper (Szeglowski et al, 1977). The last of these works involved complementary radiochemical studies to confirm the electrochemical findings. The authors concluded that "*flotation phenomena ... must be discussed in conjunction with sorption processes, and not, as is common, on the basis of thermodynamic properties of bulk phases only*". Kowal and Pomianowski (1973) concluded that "*the shift in the prepeak potentials towards negative values with respect to the potentials of the bulk reactions underlines the role of electrosorption in the process of collector binding by a mineral surface*". We arrived at similar conclusions (Woods, 1971, 1996) regarding the importance of chemisorbed layers deposited at underpotentials to the development of the metal/collector compound. With a number of co-workers, we have fitted chemisorption coverage data to the Frumkin adsorption isotherm and elucidated the chemisorption process with complementary XPS and FTIR investigations (*see* Woods, 1996). Since chemisorption occurs at underpotentials, it is the thermodynamically favoured process. This process offers the most effective utilization of the collector because a monolayer forms before the nucleation and growth of the bulk phase. The potential at which a finite contact angle is established, and flotation is initiated, has been found to correspond to the chemisorption region (Woods, 1996). Usually, significant flotation recovery is observed at low thiol coverage, about 50% recovery at a fractional coverage of ~0.2, and maximum recovery at a coverage of about half a monolayer.

Buckley et al (1997) applied SERS to verify the integrity of ethyl xanthate chemisorbed on silver and hence to resolve controversy that existed regarding the interpretation of XPS and FTIR data. Woods and Hope (1998) and Woods et al (1998a,b) carried out further studies on the chemisorption of ethyl xanthate on silver and extended these investigations to include copper and gold surfaces. In each case, the SERS spectra confirmed that ethyl xanthate retains its molecular integrity when it is adsorbed on these metals and that chemisorption occurs at underpotentials to the formation of the bulk compound which is the metal xanthates in the case of copper and silver, and dixanthogen for gold. Hope et al (2001a) found that similar behaviour was observed for isopropyl, isobutyl and isoamyl xanthates on silver. In these studies, it was shown that the chemisorption prewave on voltammograms shifted to more negative values by 0.028 V for each additional carbon atom in the alkyl chain. This value is consistent with the data of Kakovsky (1957) for the effect of alkyl chain length on the solubility product of silver xanthates and hence indicates that similar underpotentials for chemisorption apply to each xanthate homologue.

SERS studies on the interaction of *O*-isopropyl-*N*-ethylthionocarbamate (IPETC) with copper surfaces (Woods and Hope, 1999) showed that this collector also chemisorbs at underpotentials to Cu(IPETC) formation. Adsorption involved a charge transfer process in which the sulfur atom in the organic species becomes bonded to a copper atom in the metal surface and the hydrogen is displaced from the nitrogen atom to form a hydrogen ion in solution.

SERS investigations of the interaction of 2-mercaptobenzothiazole (MBT) with silver, gold and copper electrodes in aqueous solutions of pH 4.6 and 9.2 showed that the collector was adsorbed at all potentials studied (Woods et al, 2000). Rest potential measurements did not yield the reversible potentials for the formation of the metal compounds because the systems were electrochemically highly irreversible. Adsorption was shown to occur through a charge transfer process in which MBT becomes bonded to silver atoms in the surface through the exocyclic sulfur atom. Most Raman bands appeared at the same positions as those in the metal compounds, but the band arising from the NCS stretching mode was blue-shifted by $\sim 10 \text{ cm}^{-1}$. This shift was considered to be indicative of chemisorption with the shift being explained in terms of the absence in the monolayer of the intermolecular bonding that occurs in the bulk compound.

Spectroelectrochemical investigations have been made on the suppression of silver dissolution in alkaline cyanide solutions by MBT (Hope et al, 2001b) and by diisobutyl dithiophosphinate (DIBDTPI) (Hope et al, 2001c). The objective of these studies was to determine the extent to which a flotation collector could diminish silver losses in flotation when cyanide is used as a depressant. Voltammograms in the positive-going direction recorded for a silver electrode in solutions of pH 11 containing $10^{-2} \text{ mol dm}^{-3} \text{ CN}^{-}$ together with different DIBDTPI concentrations following conditioning in the test solution for 10 min or 2 h are presented in Fig. 1.

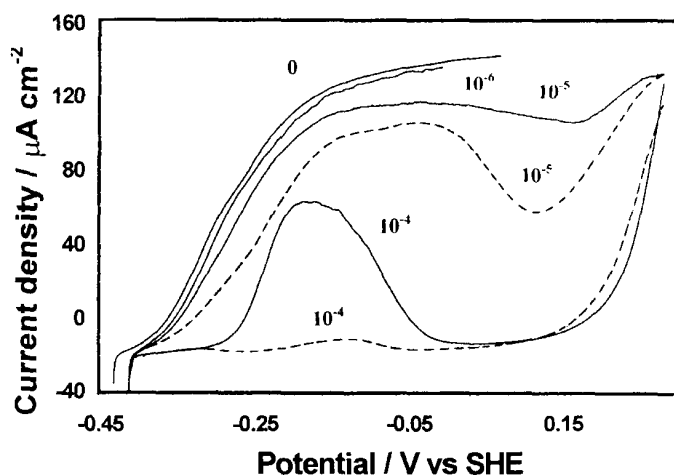


Fig. 1. Polarization curves at 0.5 mV s^{-1} in the positive-going direction for silver in deaerated solutions of the pH 11 buffer containing $10^{-2} \text{ mol dm}^{-3} \text{ CN}^-$ together with 0 , 10^{-6} , 10^{-5} , or $10^{-4} \text{ mol dm}^{-3}$ DIBDTPI. Silver electrode immersed in a solution of the same composition in equilibrium with air for ——— 10 min and - - - - 2h prior to transfer to the electrochemical cell

In the absence of the collector, the current for dissolution of silver in the cyanide solution increases to a mass transport controlled limiting current. In the presence of DIBDTPI, dissolution is inhibited, the inhibition increasing with increase in DIBDTPI concentration and conditioning time. That the inhibition results from adsorption of DIBDTPI was confirmed by SERS spectra. Figure 2 shows a spectrum from a silver electrode at the corrosion potential compared with a Raman spectrum from AgDIBDTPI.

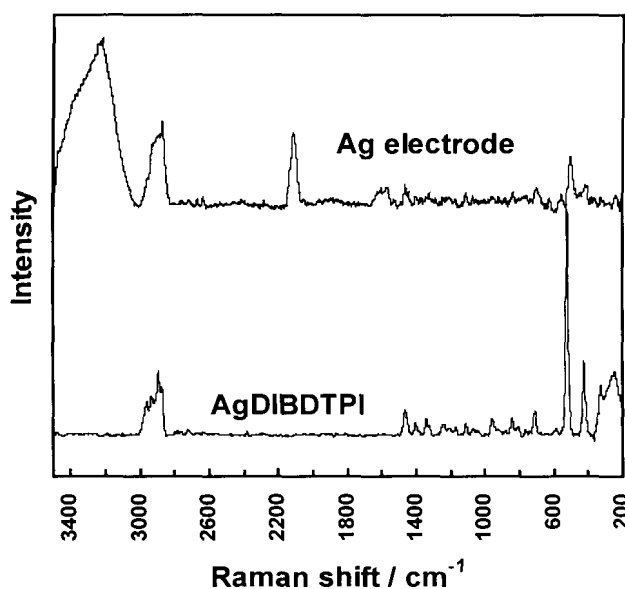


Fig. 2. Raman spectra for AgDIBDTPI and SERS spectrum from a silver electrode in pH 11 solution containing $10^{-2} \text{ mol dm}^{-3} \text{ CN}^-$ together with $10^{-4} \text{ mol dm}^{-3}$ DIBDTPI in equilibrium with air at the open circuit potential

The band at 522 cm^{-1} for AgDIBDTPI is assigned to the PS_2 stretching vibration; most of the other bands arise from vibrations within the isobutyl groups. In particular, the bands near 2800 cm^{-1} arise from stretching vibrations of carbon-hydrogen bonds in the hydrocarbon chain. It can be seen from Fig. 2 that the SERS spectrum from the silver electrode displays all the bands exhibited by the silver compound and hence DIBDTPI is bonded to Ag atoms in the silver surface. The spectrum also displays a band at 2114 cm^{-1} which is assigned to the $\text{C}\equiv\text{N}$ stretching vibration from cyanide bonded directly to silver atoms in the surface or to adsorbed silver cyano-complexes.

The interaction of DIBDTPI has also been investigated in the absence of cyanide. SERS spectra were observed for a silver electrode in $10^{-4}\text{ mol dm}^{-3}$ DIBDTPI at pH 9.2 at all potentials investigated. Spectra were recorded *in situ* at controlled potential, on emersed electrodes, and *ex situ* after washing the electrode surface with pure water. A selection of the spectra is shown in Fig. 3.

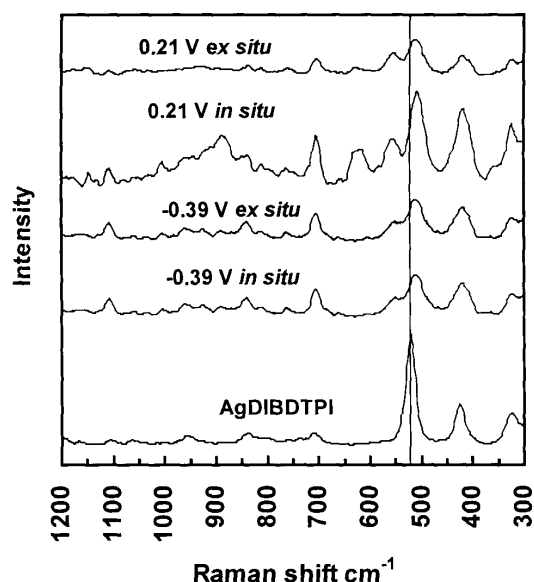


Fig. 3. SERS spectra in the low wavenumber region from a silver electrode in $10^{-4}\text{ mol dm}^{-3}$ DIBDTPI solution of pH 9.2 held for 5 min at -0.39 and 0.21 V recorded *in situ* and *ex situ*. Vertical line is the position of the PS_2 band stretch vibration for AgDIBDTPI

For potentials $\geq -1\text{ V}$, the SERS spectra were the same as the Raman spectrum for AgDIBDTPI except that the band arising from the PS_2 stretching vibration is blue-shifted by $\sim 20\text{ cm}^{-1}$, and an additional band is observed at 556 cm^{-1} . The observed blue shift is consistent with the surface species being chemisorbed. As pointed out above, a similar shift was observed for MBT (Woods et al, 2000). The fact that the SERS spectra were also observed *ex situ* after rinsing the electrode surface confirms that the surface species was chemisorbed and was not present as a specifically adsorbed ion.

In addition, Raman spectra were recorded after polarisation in the region in which voltammetry had shown AgDIBDTPI to develop. After polarisation for 5 min, the PS_2

stretch band appeared at the same wavenumber as it did at lower potentials. On extended polarisation, two bands became apparent, one at the chemisorption position and the other corresponding to that for AgDIBDTPI. Eventually, the latter band became dominant. This is the behaviour expected for the development of a AgDIBDTPI phase covering an initial chemisorbed layer.

No SERS spectra were evident with copper electrodes in the presence of DIBDTPI, but the formation of CuDIBDTPI was confirmed from Raman spectra at potentials at which an anodic current is observed on voltammograms. The absence of a SERS spectrum can not be taken as evidence that DIBDTPI does not chemisorb on copper sulfide minerals since similar results were observed with diethyldithiophosphate (DTP) on copper. It has been established (Woods, 1996) that DTP chemisorbs on chalcocite and this indicates that copper metal does not behave in the same manner as copper sulfide minerals with regard to interaction with thiophosphate collectors. In this regard, thiophosphorous collectors differ from the other collectors studied by Raman spectroelectrochemistry. At potentials at which DIBDTPI oxidizes to (DIBDTPI)₂ on gold, Raman spectra were observed from the disulfide and AuDIBDTPI. SERS spectra were also found on gold under laser illumination that were characteristic of the development of layer of sulfur and this is explained in terms of photolysis of DIBDTPI radicals formed as intermediates in the oxidation of DIBDTPI to its disulfide.

HYDROMETALLURGY

Leaching of sulfide minerals is important in both the recovery of metal values from ores and in environmental concerns associated with mining. Passivation of the sulfide surface is important in both these situations. In the former case, avoiding passivation is the key to improving leach performance. Raman spectroscopy has been applied by Wadsworth and co-workers (Zhu et al, 1992; Turcotte et al, 1993; Li et al, 1993; Li and Wadsworth, 1993; Zhu et al, 1997) for the *in situ* identification of elemental sulfur and polysulfides formed on the surface of sulfide minerals. A significant thickness of product is required before normal Raman spectroscopy can detect surface species.

Gold and silver are ideal surfaces for Raman studies since they exhibit surface enhancement. The leaching of these precious metals using cyanide has been carried out since the cyanidation of low-grade ore was commercialised following MacArthur and the Forrest brothers patenting the process in 1887. Gold metal in the ore is oxidised to form the Au(CN)₂⁻ complex in aqueous solution. This process has been shown to be electrochemical in nature, an anodic gold dissolution process to form the complex ion being coupled to the cathodic reduction of oxygen. Thus, electrochemical techniques provide a means of studying directly the gold dissolution process. The kinetics of the gold-cyanide reaction is critical to the economic leaching of gold ore, and there has been a wide disparity in the results published on the rate of dissolution. Jeffrey and Ritchie (2000) provided convincing evidence that the variation in results is

due to differences in system purity, the presence of lead or silver ions, in particular, enhancing the leaching rate. They postulated that, under conditions of high purity, the gold surface is passivated by a film of a gold cyanide species and, on the basis of electrochemical measurements, argued that the passivating layer must be disrupted by the presence of impurity species.

We are, at present, carrying out Raman spectroelectrochemical studies on the dissolution of gold in different leachants. We have found that recording Raman spectra in real time together with cyclic voltammograms is a useful approach for studying this system and term this procedure CV Raman spectroscopy. A cyclic voltammogram at 10 mV s^{-1} from a gold electrode in a pH 11 buffer solution containing 0.01 mol dm^{-3} sodium cyanide is shown in Fig.4. SERS spectra in the frequency range in which the band for the $\text{C}\equiv\text{N}$ stretch appears, recorded during the running of voltammogram, are also presented; spectra recorded on the positive-going scan are shown above the voltammogram, and those recorded on the return scan, below. The SERS spectra are in a 3-dimensional format, with Raman shift being the z-scale and scattering intensity the y-scale. The x-scale is potential and corresponds to that for the voltammogram. CV Raman spectra were also recorded in the lower wavenumber regions where the Au-O, Au-C and Au-N stretching vibrations occur.

It can be seen from Fig. 4 that cyanide is present on the gold surface at the low potential limit. As the potential is scanned in the positive going direction, the intensity of the cyanide band increases. The band position becomes red-shifted by $\sim 35 \text{ cm}^{-1}$ per volt between -1.4 and 0 V . This Stark tuning could arise from both chemical and electrostatic effects on the surface bonding, which may be accompanied by alteration of surface binding energetics and preferred binding geometries (Weaver and Wasileski, 2000).

When the potential reaches $\sim -0.8 \text{ V}$ in Fig. 4, an anodic current is observed on the voltammogram due to dissolution of gold as $\text{Au}(\text{CN})_2^-$. At this potential, the appearance of a SERS band was observed in the frequency region in which stretching vibrations of bonds between gold and cyanide are expected. At $\sim -0.6 \text{ V}$, the current corresponding to gold dissolution becomes inhibited. It can be seen from Fig. 4 that the intensity of the $\text{C}\equiv\text{N}$ stretching band reaches a maximum at this potential. The decrease in intensity as the potential is increased further could result from the formation of a polymeric gold cyanide overlayer as suggested by Jeffrey and Ritchie (2000). The shift in the $\text{C}\equiv\text{N}$ stretching band position diminishes above 0 V and becomes close to zero in the region 0.4 to 0.6 V . This indicates that there is no longer a change in the orientation or constitution of the surface cyanide species.

The dissolution current increases again above 0.3 V , but reaches a second maximum at $\sim 0.6 \text{ V}$. The $\text{C}\equiv\text{N}$ stretching band is diminished at this peak potential and bands become apparent in the region expected for Au-O stretching vibrations. Similar Au-O bands were observed above 0.6 V by CV Raman for gold electrodes in the absence of cyanide and this substantiates identification in terms of the formation of surface oxygen species. It is evident that the surface oxide inhibits gold dissolution.

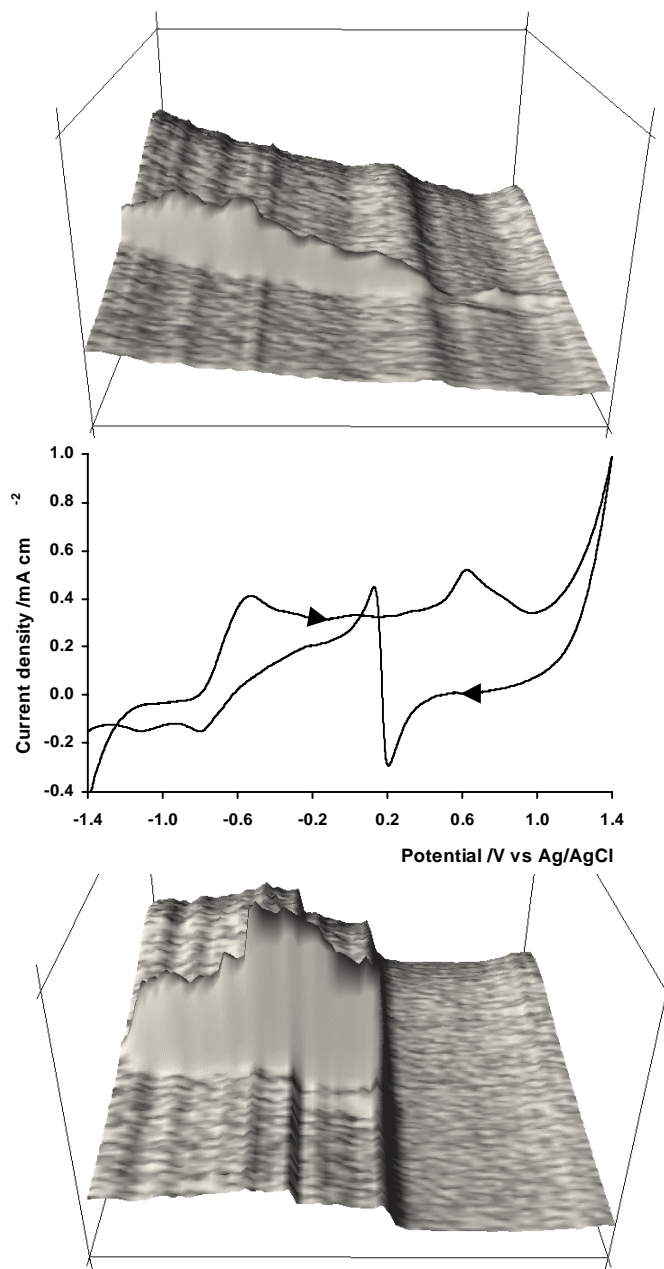


Fig. 4. CV Raman at 10 mV s^{-1} from a gold electrode in $0.01 \text{ mol dm}^{-3} \text{ CN}^-$ at pH 11

On the return scan, a cathodic current resulting from stripping of the oxide commences at ~ 1.2 V and peaks at 0.2 V. There was a corresponding decrease in the intensity of the Au-O SERS band. Just below 0.2 V, the current switches from cathodic to anodic and this is explained by gold dissolution occurring again as the surface oxygen species are removed. The re-appearance of the $C\equiv N$ stretching band at this potential (Fig. 4) confirms this interpretation. The current diminishes as the scan proceeds and this indicates that the cyanide species responsible for the SERS spectrum is the inhibiting species. This is consistent with the cyanide band position at 0.2 V being the same as that at the corresponding potential on the positive going scan. A corresponding Stark shift is observed on the negative-going scan resulting in the $C\equiv N$ stretching band returning to the same position at the end of the cycle as it occupied initially. The two small cathodic current peaks that appear at potentials below -0.8 V can be assigned to redeposition of gold from gold cyanide complexes remaining near the electrode surface. It is interesting to note that there are significant changes in the background fluorescence spectrum with change in potential (Fig. 4). These changes provide additional information on the nature of the gold surface during the potential cycle.

ELECTROMETALLURGY

Electrowinning is the most effective method for the large-scale production of pure, marketable metal in hydrometallurgical processes. Electrorefining constitutes the final polishing stage in pyrometallurgical processing. Metals such as zinc, copper and lead, that have low electrodeposition overpotentials, have a propensity to form coarse, rough deposits in such electrodeposition processes. This is due to the slow nucleation rates at low overpotentials, which compels the new metal to grow on few nuclei. To overcome this problem, various additives are included in the solution and adsorb on the metal surface, preferentially at the most active growth sites. Ideally, these additives should not become incorporated into the deposit to any significant extent, since this would diminish product quality.

SERS has been applied by a number of authors (see Buckley et al, 2002 for review) to elucidate the interaction of the additive thiourea with copper and silver surfaces in sulfate-, acid- and halide-containing solutions. In the absence of additives, Brown and Hope (1995) found that sulfate, but not bisulfate, was adsorbed on copper from sulfuric acid solutions, even though bisulfate is the predominant anion in solution.

We have recently revisited the electrodeposition of copper from sulfuric acid media taking advantage of the advances in sensitivity and capability of modern Raman instruments. The improvement in instrument performance allows real-time recording of spectra during potential excursions. The application of modern instrumentation has provided the means for detecting transient adsorption of sulfate during copper electrodeposition.

A Raman spectrum obtained from $CuSO_4 \cdot 5H_2O$ is shown in Fig. 5. The major feature is a band at 983 cm^{-1} due to the symmetrical stretching vibration of the SO_4^{2-}

group. Bending and antisymmetric stretching vibrations of sulfate give rise to the band at 615 cm^{-1} , and the band at 465 cm^{-1} is assigned to a bending mode. Fig. 5 also presents a Raman spectrum from 1 mol dm^{-3} sulfuric acid; it displays corresponding sulfate bands at 983 cm^{-1} , 595 cm^{-1} and 434 cm^{-1} together with bands at 1050 cm^{-1} and 898 cm^{-1} arising from stretching vibrations of the SO_3 group and the OH group components of the bisulfate. It is clear from Fig. 5 that Raman spectroscopy can readily distinguish between sulfate and bisulfate.

A typical spectrum from a copper surface in 1 mol dm^{-3} sulfuric acid at potentials in the region of stability of the metal is also shown in Fig. 5. The spectrum displays bands of low intensity at the same wavenumbers as expected from the 1 mol dm^{-3} sulfuric acid electrolyte itself, and hence involves both sulfate and bisulfate species. This spectrum could have arisen from the solution in the roughened electrode surface or from adsorbed species.

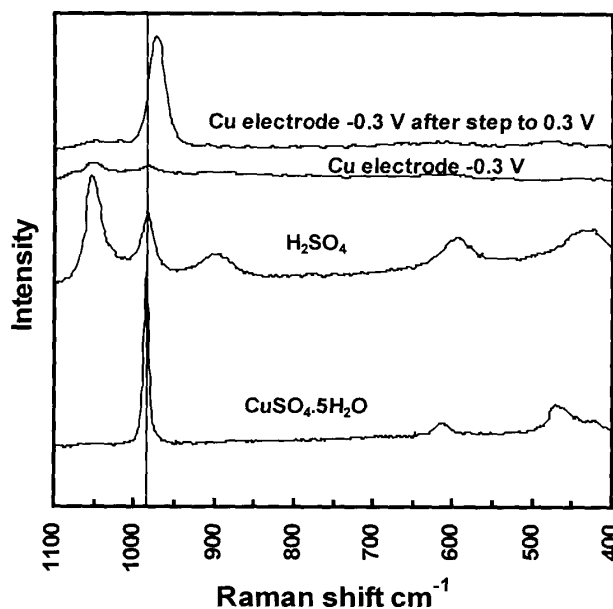


Fig. 5. Raman spectra from $\text{CuSO}_4 \cdot 5\text{H}_2\text{O}$, $1\text{ mol dm}^{-3}\text{ H}_2\text{SO}_4$, copper electrode at -0.3 V in $1\text{ mol dm}^{-3}\text{ H}_2\text{SO}_4$ and a copper electrode at -0.3 V following a potential step to 0.3 V . Vertical line is 983 cm^{-1} , which is the position of the sulfate symmetrical stretch band for CuSO_4 and H_2SO_4 .

When the potential of the copper electrode was taken into the dissolution region and then returned to the region of stability, either on a potential scan or a potential step function, SERS spectra were observed, a typical example of which is shown in Fig. 5. This spectrum has a single band at 972 cm^{-1} , which is assigned to a surface sulfate species.

The adsorbed sulfate spectrum disappeared over a period of a few minutes when the potential was held in the metal stability region. This indicates that the adsorbed sulfate is a transient species associated with copper being deposited. The intensity of the sulfate band decays due to diminution of copper plating as copper(II) ions are depleted in the vicinity of the electrode surface. The decline in intensity is not due to a

change in focus of the Raman probe resulting from copper deposition because the spectrum did not diminish in intensity when copper sulfate was added to the 1 mol dm^{-3} sulfuric acid electrolyte. The sulfate band appeared at all potentials in the Cu^0 stability region following an excursion to dissolution potentials or the addition of copper ions. It displayed only slight Stark tuning, being red-shifted by $\sim 5 \text{ cm}^{-1} \text{ V}^{-1}$ between 0.1 V and -0.5 V .

Sulfate ions have also been shown (Watanabe et al, 1995) to co-adsorb in the underpotential deposition (UPD) of copper on platinum and gold and that it is sulfate and not bisulfate that is on the surface (Shi et al, 1994). The structure and composition of copper ad-layers have been extensively studied by a variety of experimental techniques and it is well established that a honeycomb ($\sqrt{3} \times \sqrt{3}$) phase is formed in UPD Cu on Au(111) consisting of $2/3$ monolayer of Cu and $1/3$ monolayer of SO_4 . The copper is considered (Legault et al, 1996) to have a partial positive charge and this induces the adsorption of sulfate anions which themselves become partially discharged.

It is possible that the initial copper deposit formed on copper retains a partial charge analogous to that for UPD copper layers and, similarly, induces the co-adsorption of sulfate ions into the surface. The subsequent discharge of the partially charged copper atoms would complete the electrode reaction and the surface layer would reconstruct to form the stable copper structure. The sulfate ions would then be desorbed.

The SERS spectrum displays only the symmetrical stretching vibration of sulfate; the antisymmetrical vibrations are suppressed. This would indicate that each SO_4 is sited with three oxygen atoms close to surface copper atoms with the fourth vertically above the surface. The symmetrical stretching band is blue-shifted by $\sim 11 \text{ cm}^{-1}$ from the corresponding band from H_2SO_4 or hydrated CuSO_4 . This could arise from bonding between the adsorbed sulfate and surface copper atoms.

The sulfate band did not appear on similar experiments in which the 1 mol dm^{-3} sulfuric acid solution contained 10 ppm chloride. This suggests that the transient adsorbed sulfate ions are replaced by chloride ions in the growing copper electrodeposit.

When thiourea is present in the sulfuric acid solution, SERS spectra from the organic species can readily be characterised. Hope and co-workers (Brown et al, 1995; Brown and Hope 1996; Hope and Brown, 1994) noted that the adsorption of sulfate takes place together with thiourea on copper and concluded that adsorption was a co-operative rather than a competitive process, since the intensity of the sulfate bands as well as those of thiourea, increased with increase in thiourea concentration. Furthermore, the sulfate symmetrical stretch band was found to be significantly shifted from the corresponding band in thiourea-free solution.

Hope and co-workers (Bott et al, 1998) characterized complexes formed between copper(I), thiourea, and anions such as sulfate. They determined the crystal structure of the previously unknown $[\text{Cu}_4(\text{tu})_7](\text{SO}_4)_2 \cdot \text{H}_2\text{O}$ (where tu is thiourea) and the

vibrational spectra of a range of copper(I) thiourea complexes. The copper atoms were found to lie in a tetrahedral arrangement forming $[\text{Cu}_4(\text{tu})_7]^{4+}$ clusters interlinked by sulfate ions, which strongly interact with thiourea ligands through hydrogen bonds. The bond lengths about the thiourea ligands indicated a decrease in the carbon–sulfur double-bond character, consistent with the co-ordination of thiourea with copper being through the sulfur atoms. The Raman bands in the sulfate complexes were found to appear at similar wavenumbers to those of the SERS bands for the species adsorbed on copper. The stretching vibration for Cu-S for these complexes was found to show a strong dependence on the copper coordination environment and the value observed in the SERS indicated that the co-ordination number for the Cu/thiourea species at the metal surface is relatively low. This is what is to be expected for a surface analogue of a copper(I) thiourea sulfate complex.

We have recently confirmed these findings with modern Raman instrumentation. A SERS spectrum from a copper electrode in 5 ppm thiourea, $1 \text{ mol dm}^{-3} \text{ H}_2\text{SO}_4$ recorded at 0 V following a 10 s potential pulse to 0.3 V is shown in Fig. 6; together with Raman spectra from $[\text{Cu}_4(\text{tu})_7](\text{SO}_4)_2 \cdot \text{H}_2\text{O}$ and from a 1 mol dm^{-3} aqueous thiourea solution.

The thiourea spectrum is characterised by bands arising from skeletal deformation/C-S stretch at 490 cm^{-1} and C=S stretch at 743 cm^{-1} (Brown et al, 1995). The spectrum from the copper thiourea sulfate crystal displays bands due to sulfate symmetrical stretch (977 cm^{-1}), C-S stretch (712 cm^{-1}), SCN bend (482 cm^{-1}), NCN bend (423 cm^{-1}) and CuS stretch (252 cm^{-1}) (Bott et al, 1998). The C=S vibration observed with thiourea itself is absent in the complex because the sulfur atoms of thiourea are now bonded to copper atoms. The SERS spectrum from the copper electrode shows that the surface species formed on copper is not thiourea itself, but is similar to that for the copper thiourea complex. All the bands observed from the complex appear in the SERS spectrum, but some are blue-shifted by $\sim 10 \text{ cm}^{-1}$. There is also a bisulfate band at 1055 cm^{-1} apparent in the SERS spectrum in Fig. 6, and this indicates that bisulfate as well as sulfate can be involved in complex formation at the copper surface. Brown et al (1995) found that the relative intensity of the bisulfate band to the other bands decreased with increase in thiourea concentration, whereas that from sulfate increased.

Brown and Hope (1996) applied *in situ* SERS spectroscopy to investigate the influence of chloride ion on the co-adsorption of thiourea and sulfate ions in sulfuric acid solution at the concentration levels used in the electrorefining of copper. They found chloride also to co-adsorb and that adsorption of the halide was favoured at low negative potentials. The presence of the chloride in solution at low concentrations was also found to result in enhancement of the adsorption of thiourea and sulfate. Furthermore, the adsorption of chloride at the copper electrode altered the molecular structure of the interface due to an interaction with co-adsorbed thiourea and sulfate species at the electrode surface.

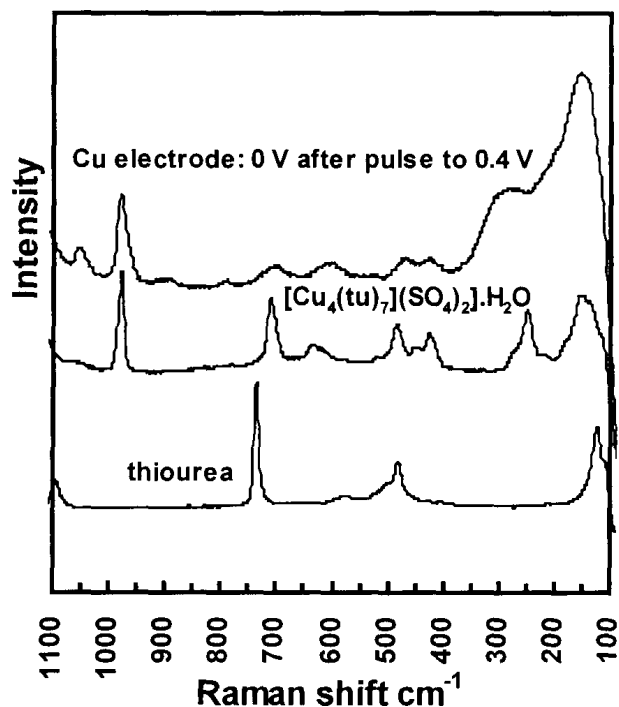


Fig. 6. Raman spectra from thiourea and from $[\text{Cu}_4(\text{tu})_7](\text{SO}_4)_2 \cdot \text{H}_2\text{O}$ and a SERS spectrum from a copper electrode at 0V after a 10 s potential pulse to 0.3 V

Brown and Hope (1996) considered that the chloride interacts with the nitrogen containing groups of the thiourea molecule adsorbed at the electrode surface as evidenced by changes in band shape and intensity for the NH_2 torsion and C-N stretching vibrational modes. In this manner, the adsorption of chloride results in a rearrangement or alteration of the molecular structure at the electrode surface that is observed by changes in signal intensity for the various vibrational bands associated with the adsorption of thiourea, sulfate and chloride at the electrode surface. These findings are consistent with adsorption of the organic molecule on the copper electrode occurring by co-ordination with the sulfur atom.

ACKNOWLEDGEMENTS

This project was supported by the Australian Research Grants Scheme. Flotation collectors were generously provided by Cytec Industries Inc.

REFERENCES

- BOTT, R. C., BOWMAKER, G.A., DAVIS, C.A., HOPE, G.A. and JONES, B.E. (1998), *Crystal structure of $[\text{Cu}_4\text{tu}_7](\text{SO}_4)_2 \cdot \text{H}_2\text{O}$ and vibrational spectroscopic studies of some copper (I) thiourea complexes*, *Inorganic Chemistry*, Vol. 37, 651-657.

- BROWN G.M. and HOPE, G.A. (1995) *In-situ spectroscopic evidence for the adsorption of SO_4^{2-} ions at a copper electrode in sulfuric acid solution*, J. Electroanal. Chem., Vol. 382, 179-182.
- BROWN G.M. and HOPE, G.A. (1996), *Confirmation of thiourea/chloride ion co-adsorption at a copper electrode by in situ SERS spectroscopy*, J. Electroanal. Chem., 413 (1996) 153-160.
- BROWN, G.M., HOPE, G.A., SCHWEINSBERG D.P. and FREDERICKS, P.M. (1995), *SERS study of the interaction of thiourea with a copper electrode in sulphuric acid solution*, J. Electroanal. Chem., 380 (1995) 161-166.
- BUCKLEY A.N. and WOODS, R. (1996), *Relaxation of the lead-deficient sulfide surface layer on oxidized galena*, J. Appl. Electrochem., Vol. 26, 899 - 907.
- BUCKLEY, A.N., HOPE, G.A. and WOODS, R. (2002), *Metals from sulfide minerals: the role of adsorption of organic reagents in processing technologies*, Solid-Liquid Interfaces Macroscopic Phenomena - Microscopic Understanding (K. Wandelt and S. Thurgate, Eds) Topics in Applied Physics, Vol. 85, Springer; Germany, pp. 59-94.
- BUCKLEY, A.N., PARKS, T.J., VASSALLO, A.M. and WOODS, R. (1997), *Verification by surface enhanced Raman spectroscopy of the integrity of xanthate chemisorbed on silver*, Int. J. Miner. Process., Vol. 51 303-313.
- FLEISCHMANN, M.; HENDRA, P. J. and McQUILLAN, A. J. (1974), *Raman spectra of pyridine adsorbed at a silver electrode.*, Chem. Phys.Lett. , **26**, 163-166.
- FLEISCHMANN, M., SOCKALINGUM, D. and MUSIANI, M.M. (1990), *The use of near infrared Fourier Transform techniques in the study of surface enhanced Raman spectra*, Spectrochim. Acta, Vol. A46, 285-294.
- HOPE, G.A. and BROWN, G.A. (1994) *In-situ additive monitoring during copper deposition in acid sulfate electrolyte*, Proc. Int. Symp. Electrochemistry in Mineral and Metal Processing, (R. Woods, F.M. Doyle and P. Richardson, Eds.), PV 96-6, Electrochem. Soc., Pennington, NJ., pp. 429-438
- HOPE, G.A., WATLING, K. and WOODS, R. (2001a), *A SERS spectroelectrochemical investigation of the interaction of isopropyl, isobutyl and isoamyl xanthates with silver*, Colloids and Surfaces A, Vol. 178 157-166.
- HOPE, G.A., WATLING, K. and WOODS, R. (2001b), *An electrochemical investigation of the suppression of silver dissolution in aqueous cyanide by 2-mercaptobenzothiazole*, J. Appl. Electrochem. , Vol. 31, 703-709.
- HOPE, G.A., WOODS, R. and WATLING, K. (2001c), *A spectroelectrochemical investigation of the influence of sodium diisobutylidithiophosphate on silver dissolution in aqueous cyanide*, J. Appl. Electrochem. Vol. 31, 1285-1291.
- JEFFREY, M.I. and RITCHIE, I.M. (2000), *The leaching of gold in cyanide solution in the presence of impurities I. The effect of lead*, J. Electrochem. Soc., Vol. 147 3257-3262.
- KAKOVSKY, I.A. (1957), *Physicochemical properties of some flotation reagents and their salts with ions of heavy non-ferrous metals*, Proc. 2nd Int. Congr. Surface Activity, Vol. IV, (J.H. Schulman, Ed.), Butterworth, London, pp. 225-237.
- KOWAL, A. and POMIANOWSKI, A. (1973), *Cyclic voltammetry of ethyl xanthate on a natural copper sulphide electrode*, J. Electroanal. Chem., Vol. 46, 411-420.
- LEGAULT, M., BLUM L. and HUCKABY, D.A. (1996), *An extended hexagon model for Cu underpotential deposition on Au(III)*, J. Electroanal. Chem., Vol. 409, 79-86.
- LI, J., ZHU, X. and WADSWORTH, M.E. (1993), *Raman spectroscopy of natural and oxidized metal sulfides*, EPD Congress, (J.P. Hager, Ed.) MME/AIME, Warrendale PA, pp.229-243.
- LI, J. and WADSWORTH, M.E. (1993), *Raman spectroscopy of electrochemically oxidized pyrite and optimum conditions for sulfur formation*, Hydrometallurgy: Fundamentals, Technology and Innovation, (J.B. Hiskey and G.W. Warren, Eds.) SME/AIME, Littleton, CO, pp.127-141.
- NIXON, J.C. (1957), *Discussion*, Proc. 2nd Int. Congr. Surface Activity, Butterworth, London, Vol. 3, p.369.
- POMIANOWSKI, A. (1967), *Cyclic voltammetry in dilute solutions of potassium ethyl xanthate*, Roczniki Chem., Vol. 41, 1125-1129.

- SHI, Z. and LIPKOWSKI, J. (1994), *Coadsorption of Cu²⁺ and SO₄²⁻ at the Au(111) electrode*, J. Electroanal. Chem., Vol 365, 303-309.
- SZEGLOWSKI, Z., CZARNECKI, J., KOWAL, A. and POMIANOWSKI, A. (1977), *Adsorption of potassium ethyl xanthate on a copper electrode surface*, Trans. IMM, Vol. 86, C115-118.
- TURCOTTE, S.B., BENNER, R.E., RILEY, A.M., LI, J., WADSWORTH M.E. and BODILY, D.M. (1993), *Surface analysis of electrochemically oxidized metal sulfides using Raman spectroscopy*, J. Electroanal. Chem., Vol. 347, 195-205.
- WATANABE, M. UCHIDA H. and IKEDA, N. (1995), *Electrochemical quartz crystal microbalance study of copper ad-atoms on gold and platinum electrodes Part I. Adsorption of anions in sulfuric acid*, J. Electroanal. Chem., Vol. 380, 255-260.
- WEAVER, M.J. and WASILESKI, S.A. (2000) *Electrochemical Surface Spectroscopy*, The Electrochemical Society Interface, pp.34-36.
- WOODS, R. (1971) *The oxidation of ethyl xanthate on platinum, gold, copper, and galena electrodes: relation to the mechanism of mineral flotation*, J. Phys. Chem., Vol. 75, 354-362.
- WOODS, R. (1996) *Chemisorption of thiols on metal and metal sulfides*, Modern Aspects of Electrochemistry, No. 29, (Eds., J.O'M. Bockris, B.E. Conway and R.E. White), Plenum Press, NY, pp. 401-453.
- WOODS, R. and HOPE, G.A. (1998), *Spectroelectrochemical investigations of the interaction of ethyl xanthate with copper, silver and gold: I. FT-Raman and NMR spectra of xanthate compounds*, Colloids and Surfaces A, Vol. 137, 319-328.
- WOODS, R. and HOPE, G.A. (1999), *A SERS spectroelectrochemical investigation of the interaction of O-isopropyl-N-ethylthiocarbamate with copper surfaces*, Colloids and Surfaces A, Vol. 146, 63-74.
- WOODS, R., HOPE, G.A. and BROWN, G.M. (1998a), *Spectroelectrochemical investigations of the interaction of ethyl xanthate with copper, silver and gold: II. SERS of xanthate adsorbed on silver and copper surfaces*, Colloids and Surfaces A, Vol. 137, 329-337.
- WOODS, R., HOPE, G.A. and BROWN, G.M. (1998b), *Spectroelectrochemical investigations of the interaction of ethyl xanthate with copper, silver and gold: III. SERS of xanthate adsorbed on gold surfaces*, Colloids and Surfaces A, Vol. 137, 339-344.
- WOODS, R., HOPE, G.A. and WATLING, K. (2000), *A SERS spectroelectrochemical investigation of the interaction of 2-mercaptobenzothiazole with copper, silver and gold surfaces*, J. Appl. Electrochem., Vol. 30, 1209-1222.
- ZHU, X.; LI, J.; BODILY, D.M.; WADSWORTH, M.E. (1992), *Tranpassive oxidation of pyrite*, Proc. Int. Symp. Electrochemistry in Mineral and Metal Processing III, PV 92-17, (R. Woods and P.E. Richardson Eds.), Electrochem.Soc., Pennington, NJ., pp.391- 409.
- ZHU, X.; WADSWORTH, M.E.; WOODS, R. (1997), *Electrochemical kinetics of the anodic dissolution of nickel matte and synthetic Ni₃S₂*, Nickel-Cobalt 97, Volume I: Hydrometallurgy and Refining of Nickel and Cobalt (W.C. Cooper and I. Mihaylov, Eds.) CIM, Canada, pp. 153-167.

Hope G.A., Woods R., K. Watling K., *Badania spektrochemiczne SERS w przeróbce kopalni*, Fizykochemiczne Problemy Mineralurgii, 36, (2002) 21-38 (w jęz. ang.)

W pracy przedyskutowano zastosowania spektroskopii rozproszenia ramanowskiego (ze wzmocnieniem sygnału wskutek odbicia promieniowania od powierzchni - SERS) w badaniach związanych z procesami przeróbki minerałów w których widmo wykonywane jest *in situ*. W układach flotacyjnych zastosowano SERS do charakterystyki powłok na metalach z grupy miedzi, powstających w wyniku oddziaływania na te metale w warunkach kontrolowanego potencjału roztworów ksantogenianów: etylowego, izopropylowego, izobutyłowego i izoamylowego, a także o-izopropyl-N-etylotionocarbaminianu, 2-merkaptobenzotiazolu oraz dwuizobutylo dwutiofosfonianu. W przypadku wszystkich kolektorów adsorpcja następuje w wyniku przeniesienia ładunku z wytworzeniem wiązania metal-siarka, a jeśli znany jest odwracalny potencjał tworzenia fazy objętościowej to można stwierdzić,

że wiązanie z powierzchnią następuje przy potencjale niższym niż dla reakcji w fazie objętościowej. Zaobserwowano, że roztwarzanie srebra w zasadowych roztworach cyjankowych jest silnie spowalniane w wyniku chemisorpcji 2-merkaptobenzotiazolu i dwuizobutylo dwutiofosfonianu. W zakresie hydrometalurgii zastosowano SERS do badania ługowania złota. Stosując rejestrację widm SERS w trakcie wykonywania woltamperogramów przy zmieniającym się potencjale obserwowano zmiany w składzie warstw powierzchniowych na złocie w wyniku traktowania powierzchni złota cyjankami przy różnych potencjałach. SERS zastosowano również do badania procesów elektrometalurgicznych, stwierdzając że w procesach osadzania miedzi z kwaśnych roztworów siarczanowych bierze udział przejściowy produkt zawierający grupę siarczanową.